ELSEVIER

Biomaterials 22 (2001) 2333–2343

Biomaterials

www.elsevier.com/locate/biomaterials

Immunohistochemical characterization of axonal sprouting and reactive tissue changes after long-term implantation of a polyimide sieve electrode to the transected adult rat sciatic nerve

Petra Margarete Klinge[a], Morad Ali Vafa[a], Thomas Brinker[b], Almuth Brandis[c], Gerhard Franz Walter[c], Thomas Stieglitz[d], Madjid Samii[a,b], Konstantin Wewetzer[e,*]

[a]*Department of Neurosurgery, Hannover Medical School, 30625 Hannover, Germany*
[b]*Department of Neurosurgery, Nordstadt Hospital Hannover, 30167 Hannover, Germany*
[c]*Department of Neuropathology, Hannover Medical School, 30625 Hannover, Germany*
[d]*Fraunhofer Institute for Biomedical Engineering, Ensheimer Str. 48, 66386 St. Ingbert, Germany*
[e]*Department of Neuroanatomy, Hannover Medical School, Center of Anatomy OE4140, Carl-Neuberg-Str 1, 30625 Hannover, Germany*

Received 11 September 2000; accepted 27 November 2000

Abstract

The development of artificial microstructures suited for interfacing of peripheral nerves is not only relevant for basic neurophysiological research but also for future prosthetic approaches. Aim of the present study was to provide a detailed analysis of axonal sprouting and reactive tissue changes after implantation of a flexible sieve electrode to the proximal stump of the adult rat sciatic nerve. We report here that massive neurite growth after implantation, steadily increasing over a period of 11 months, was observed. Parallel to this increase was the expression of myelin markers like Po, whereas non-myelin-forming Schwann cells did not change. Compared to five weeks post-implantation, where both Schwann-cell phenotypes were intermingled with each other, non-myelin-forming Schwann cells occupied a peripheral position in each microfascicle after 11 months. After an initial increase, hematogenous macrophages were down-regulated in number but maintained close contact with the implant. However, at no time were signs of its degradation observed. It is concluded that the introduced flexible polyimide electrode is suitable for contacting peripheral nerves since it permits substantial neurite growth and offers excellent long-term stability.

Keywords: Biocompatibility; Sieve electrode; Polyimide; Axonal sprouting; Sciatic nerve

1. Introduction

The peripheral nervous system is generally considered a permissive environment with respect to neurite growth after injury [1,2]. Complete functional recovery in the clinical practice, however, is only observed, when nerves are severed at some distance away from the cell body. Proximal lesions, like those of the brachial plexus, still have a poor clinical prognosis [3–6]. This is due, at least in part, to the irreversible destruction of muscle tissue during the prolonged time interval in which regenerating neurites regrow towards their target tissue [1,7–9]. One experimental strategy to improve recovery after such lesions is to restore the neuromuscular junction by grafting of embryonic spinal cord and/or cortical neurons into the spinal cord or the distal part of the transected peripheral nerve [10–14]. The atrophy of muscle, however, will only be efficiently counteracted when the neuromuscular junction regains controlled activity. Putting such experimental approaches into practice will therefore not only require the grafting of neurons but also their electrical stimulation triggering muscle contraction. This may be achieved by electrodes integrated into the nerve. A number of groups have followed this approach of micromachined neural prostheses and a variety of

* Corresponding author. Tel.: +49-511-532-2895; fax: +49-511-532-2880.
E-mail address: wewetzer.konstantin@mh-hannover.de (K. Wewetzer).

0142-9612/01/$ - see front matter
PII: S0142-9612(00)00420-8

different electrode designs, such as cuff, shaft and sieve electrodes have been introduced [15–18]. Most of these studies, however, have been difficult to interpret because of their major focus on electrophysiological issues. A thorough histological analysis of the electrode's tissue integration and the molecular characterization of cells in the vicinity of an explant has so far not been performed. Characterizing electrode type-specific responses, however, is particularly important since it may contribute to modified surgical procedures and/or electrode designs.

Aim of the present study was to perform a detailed molecular characterization of axonal sprouting and reactive tissue changes after short- and long-term implantation of a flexible polyimide sieve electrode. The proximal nerve stump of the transected adult sciatic nerve was chosen as a model system, since it is well characterized with regard to its fiber composition, axonal sprouting and neuroma formation [19–21]. We used polyimide [22] since it is relatively flexible and at least as stable as silicon and has been shown to display good integration, thus avoiding the risk of secondary damage [23]. We report here that after long-term implantation, massive neurite growth took place through the sieve electrode. The number of neurites penetrating the sieve electrode steadily increased over a period of 11 months. Implantation was done without substantial secondary nerve damage and the implant was stable for at least 11 months. At the sieve electrode–nerve interface, regular myelinated and unmyelinated microfascicles were observed. After an initial up-regulation, lesion-related markers as well as hematogenous macrophages surrounding the implant were found to be down-regulated.

2. Materials and methods

2.1. Design of the sieve electrode

The polyimide (PI2611, HD Microsystems) sieve implant (10 μm thickness) had a total length of 30 mm with a ribbon cable 1 mm wide (Fig. 1a and b). The implant was circular shaped with a diameter of 2 mm. The sieve part of the interface had 657 via holes with a diameter of 40 μm (Fig. 1a and b). The interface of the present prototype carried three straps (0.5 mm wide) at its outer circumference for epineural fixation onto the nerve stump (Fig. 1b). In the present study, we used sieve electrodes devoid of substrate-integrated multi-electrode array within the sieve interface and the ribbon in order to facilitate histological processing. The device was manufactured using micromachining technologies [18,24]: spin coating for polyimide resin processing, a polyimide oven (PB 6-2, YES, San José, CAS, USA) for curing, photolithography and reactive ion etching (RIE, PC320, STS). The three straps were bent and tempered at 340°C for 1 h to remain stable in a 90° position. Since after process technology, the devices displayed some "hydrophobic" reaction during handling in physiological saline solution, they were exposed to oxygen plasma (2 min, 120 W, 40 sccm O_2) to improve the handling properties. The effect of plasma treatment was confirmed by contact angle measurements using drops of deionized water. Plasma-treated sieve implants displayed a contact angle of 20° compared to 55° of the untreated sieve implants after storage in water.

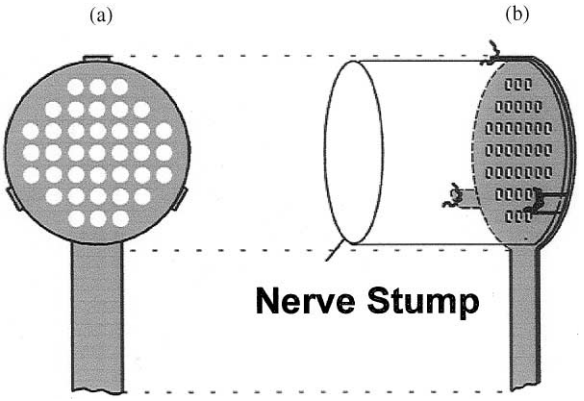

Fig. 1. Graphic scheme of the used poylimide sieve implant. The implant was 10 μm thick and 2 mm in diameter (a, b). The central part of the sieve interface consisted of 657 via holes with a mean diameter of about 40 μm (a, b). Three straps (0.5 mm wide) for epineural suturing were oriented perpendicular to the planar sieve interface (b) and displayed a distance of 120° to each other.

2.2. Experimental design and surgical procedures

The experimental design of the present study included the transection of the sciatic nerve of the adult rat followed by the implantation of the sieve electrode to the proximal nerve stump. After post-operative periods of five weeks (short-term), six, and 11 months (long-term), the sieve electrode–neuroma complex was excised, processed for histology, and immunostained using cell type-specific antibodies. Experimental animals (Institutional approval, Bezirksregierung Hannover) consisted of 15 female and male Sprague Dawley rats (250–400 g). Animals were anaesthetized with an intraperitoneal injection of Ketamine and Xylazine at a dose of 100 and 8 mg/kg body weight, respectively. The sciatic nerve was unilaterally exposed at mid-thigh level, sharply transected proximal to the bifurcation into the peroneal and sural nerves, and finally, a nerve segment was removed. The straps of the electrode were sutured onto the epineurium using a 10–0 monofilament polyamide thread. After implantation, muscle fascias were coapted prior to the wound closure. To prevent autotomy of the limb, the rats were nourished with amytryptilline added to the drinking water (0.004%) [25]. Animals were killed by an overdose of ketamine (>200 mg/kg) and xylazine (>40 mg/kg).

Lesioned animals that received no polyimide implants were not included in the present study since neuroma formation and the occurrence of immune cells after peripheral nerve injury has already been thoroughly documented by several other groups [26–29].

2.3. Tissue preparation and histological procedures

The isolated tissue was immediately cryopreserved using liquid nitrogen-cooled isopenthane and embedded in a cryomatrix. Specimens were stored at −80°C. Sections (longitudinal and transverse, 5 μm thick) were mounted on poly-L-lysine-coated slides (Sigma) and allowed to dry for 3–4 h before histochemical (hematoxylin/eosin) and immunocytochemical staining.

2.4. Immunohistochemistry

After drying, sections were rinsed in PBS. For blocking of endogenous peroxidase activity, sections were treated with 0.6% H_2O_2 diluted in methanol for 15 min. Antibodies were diluted in PBS containing 5% rat serum and 1% BSA. Primary and secondary antibodies were applied at 4°C overnight and for 1 h at room temperature, respectively. Dilution of the antibodies was as follows: antineurofilament undiluted, anti-Po-antibodies 1 : 500, anti-27C7-1 : 50, and anti-10B3-antibodies 1 : 5. Staining of macrophages was done using anti-CD11b- (1 : 50), and ED2-antibodies (1 : 500). Staining with anti-CD11b-antibodies required fixation of tissue. Prior to blocking of endogenous peroxidase, which was done in ethanol instead of methanol, sections were treated with 4% isopropanol. Primary antibodies (s. Antibodies) were either detected using the streptavidin–biotin complex system (Dako), or horseradish peroxidase-coupled secondary antibodies (Dako) according to the manufacturer's instruction with DAB as a chromogen for color development. Specificity controls included the omission of the primary antibodies.

2.5. Antibodies

Monoclonal antibodies against neurofilament reactive with the 68, 160, and 200 kDa isoforms were obtained from Linaris (clone E010, Wertheim, Germany), anti-Po antibody [30] was a generous gift from H.-J. Hartung and J.J. Archelos (Department of Neurology, University of Graz, Austria). Monoclonal 27C7- and 10B3-antibodies were generated using viable secondary Schwann cells as an immunogen and have been described elsewhere [31,32]. The spatiotemporal distribution of the 10B3 antigen during development and following nerve injury was found to be identical with tenascin-C (Wewetzer, unpublished). Macrophage-specific anti-CD11b antibodies (clone MRC Ox42) and ED2-antibodies were from Serotec (Wiesbaden, Germany).

3. Results

3.1. Sieve electrode fixation

Five weeks, six and 11 months following implantation of the sieve electrode to the proximal stump of the adult rat sciatic nerve, the location and fixation of the electrode within the neuroma formation was found to be generally consistent (not shown). In some cases only, the electrode was slightly tilted towards the longitudinal axis of the proximal nerve stump. However, the sieve interfaces were each fixed and attached to the nerve tissue. Fig. 2 shows the electrode/neuroma complex six months after implantation stained by anti-neurofilament antibodies. Microfascicles crossing the entire face of the sieve electrode can be observed. Comparison of short- and long-term implantation did not reveal any substantial differences with respect to the gross morphological appearance of the sieve electrode–neuroma complex (not shown).

3.2. The nerve–electrode transitional area

3.2.1. Axonal sprouting and Schwann cell–neuron interaction

Immunostaining for neurofilament five weeks after implantation demonstrated that microfascicles containing multiple axons had crossed the sieve electrode (Figs. 3a,

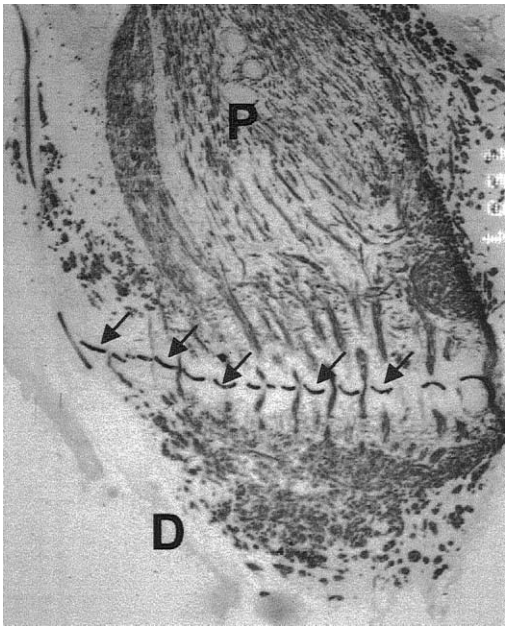

Fig. 2. Low-power photograph of the sieve electrode–neuroma complex six months after implantation. The sieve implant was well integrated and tightly fixed to the proximal nerve stump (P). Immunostaining for neurofilament revealed that microfascicles crossed the via holes to a similar extent over the entire width of the sieve implant. In the distal neuroma (D), microfascicles underwent aberrant sprouting (D). Arrows indicate the position of the electrode–sieve interface. Magnification 50×.

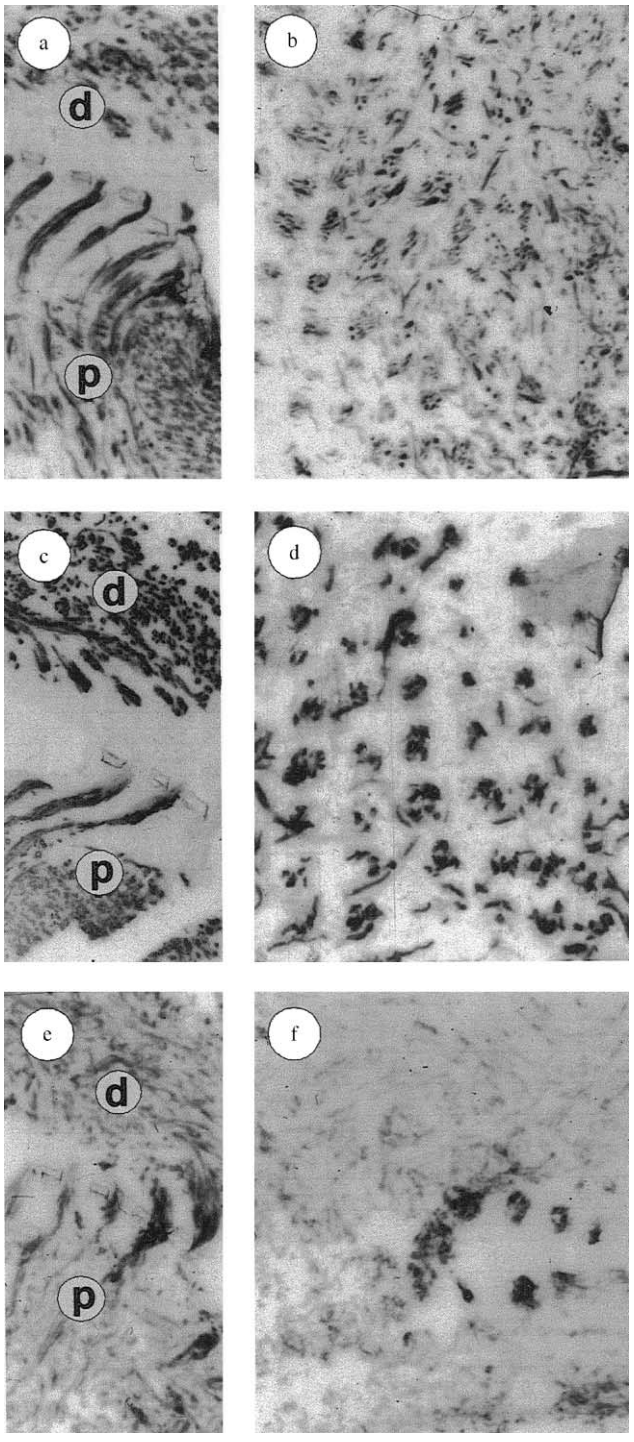

Fig. 3. Immunostaining of longitudinal (a, c, e) and transverse (b, d, f) sections of the sieve electrode–nerve complex five weeks post-operatively with antineurofilament- (a, b), anti-Po- (c, d), and 27C7-antibodies (e, f). Immunostaining for myelin- (c, d) and non-myelin-forming Schwann cells (e, f) revealed that neurites crossing the via holes (a, b) were accompanied by both Schwann-cell phenotypes. Magnification 98×; p: proximal nerve stump, d: distal neuroma.

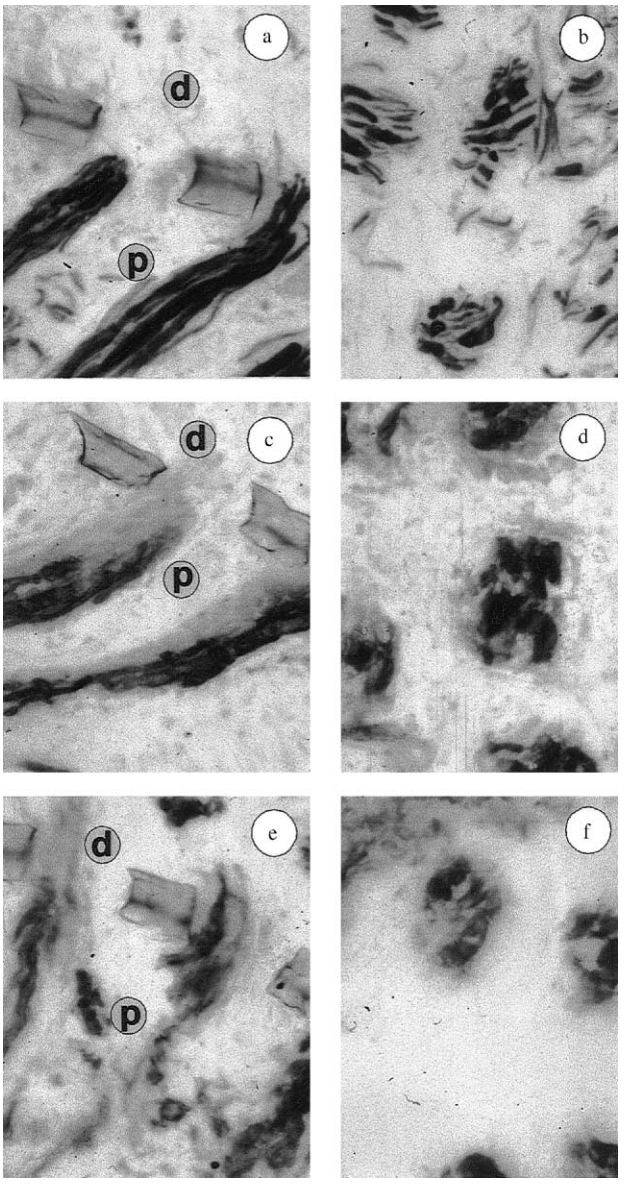

Fig. 4. High-power photographs longitudinal (a, c, e) and transverse (b, d, f) sections of the sieve electrode–nerve complex 5 weeks post-operatively stained with antineurofilament (a, b), anti-Po (c, d) and 27C7-antibodies (e, f). Myelinated and unmyelinated fibers of varying diameter (a, b) crossed the via holes at their center (a, c, e). The number of myelin-expressing Schwann cells (Po-positive, d) seemed to be slightly higher than the number of non-myelin-forming Schwann cells (27C7-positive, f). Magnification 390×; p: proximal nerve stump, d: distal neuroma.

b and 4a, b). Sprouting of axonal processes was not confined to a restricted area but was observed over the entire face of the sieve electrode. Due to the orientation of the electrode in the neuroma this was not always apparent from a single section (Fig. 3b) but was verified on serial sections (not shown). Comparison of longitudinal (Fig. 4a) and transverse (Fig. 4b) sections revealed that the neuronal processes crossed the electrode in the center of each via hole, without touching the polyimide structures. Distal to the electrode, no parallel orientation of neuronal processes was found corresponding to the

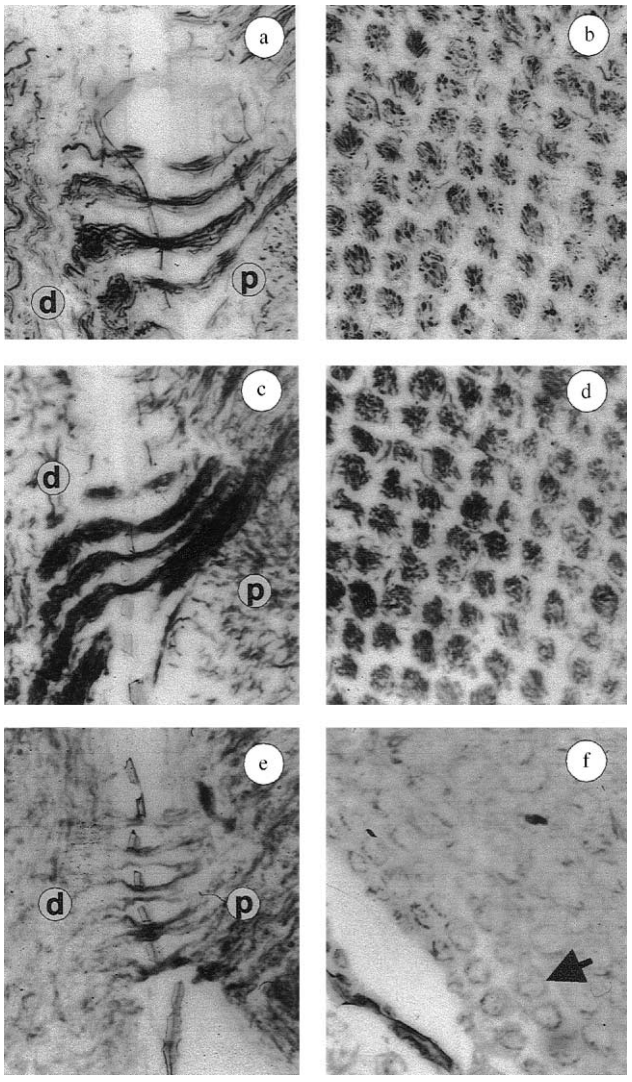

Fig. 5. Immunostaining of longitudinal (a, c, e) and transverse sections (b, d, f) of the sieve electrode–nerve complex 11 months after implantation with antineurofilament (a, b), anti-Po (c, d), and 27C7-antibodies (e, f). Compared to one month after implantation, the number of fibers positive for neurofilament (a, b) and Po (c, d) had considerably increased, whereas the number of 27C7-positive fibers seemed to remain unaltered (e, f). Immunostaining of longitudinal and transverse sections demonstrated that non-myelin-forming Schwann cells were located at the periphery of each microfascicle (f arrow), whereas neuronal processes (b) and myelin-forming Schwann cells (d) occupied a central position. The low magnification of these specimens clearly revealed that the sprouting of microfascicles occurred over the entire surface of the sieve implant. Magnification 98×; p: proximal nerve stump, d: distal neuroma.

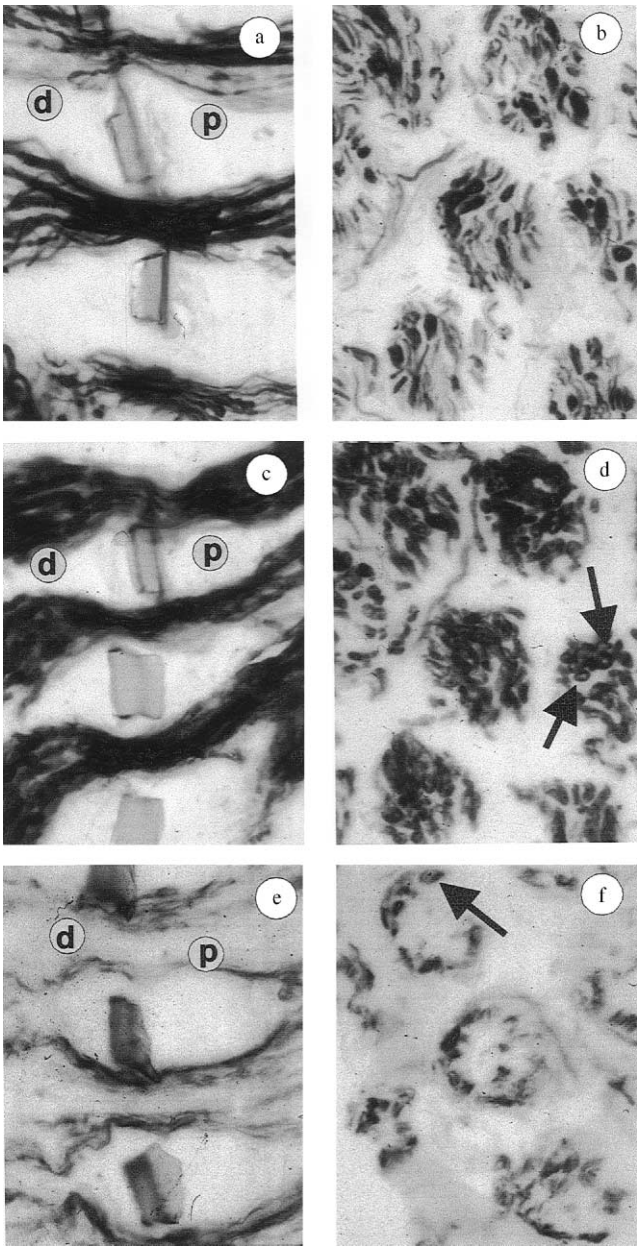

Fig. 6. High-power photographs of longitudinal (a, c, e) and transverse (b, d, f) sections of the sieve electrode–nerve complex 11 months after implantation stained with antibodies against neurofilament (a, b), Po (c, d), and 27C7 (e, f). The neuronal processes were of varying diameter (b) and crossed the via holes in a central position (a). Po-immunostaining (c, d) revealed the presence of myelinated fibers possessing circular myelin sheaths (d, arrows). Contrary to myelin-forming Schwann cells, which also occupied a central position, 27C7-positive non-myelin-forming Schwann cells (e, f) were located in the periphery of each microfascicle (f, arrow). Magnification 390×; p: proximal nerve stump, d: distal neuroma.

irregular sprouting in the neuroma (Fig. 3a). Immunoreactivity for the major peripheral myelin protein Po (Figs. 3c, d and 4c, d) and the non-myelin-forming Schwann cell marker 27C7 (Figs. 3e, f and 4e, f) demonstrated that neuronal processes were accompanied by both Schwann-cell phenotypes. Myelin-forming cells, however, seemed to outnumber the non-myelin-forming ones (Figs. 3e, f and 4e, f). Both markers were also found in the neuroma formation distal to the sieve electrode (Fig. 3c and e).

Eleven months after implantation, the number of neurofilament-positive processes crossing the sieve electrode had considerably increased. (Figs. 5a, b and 6a, b).

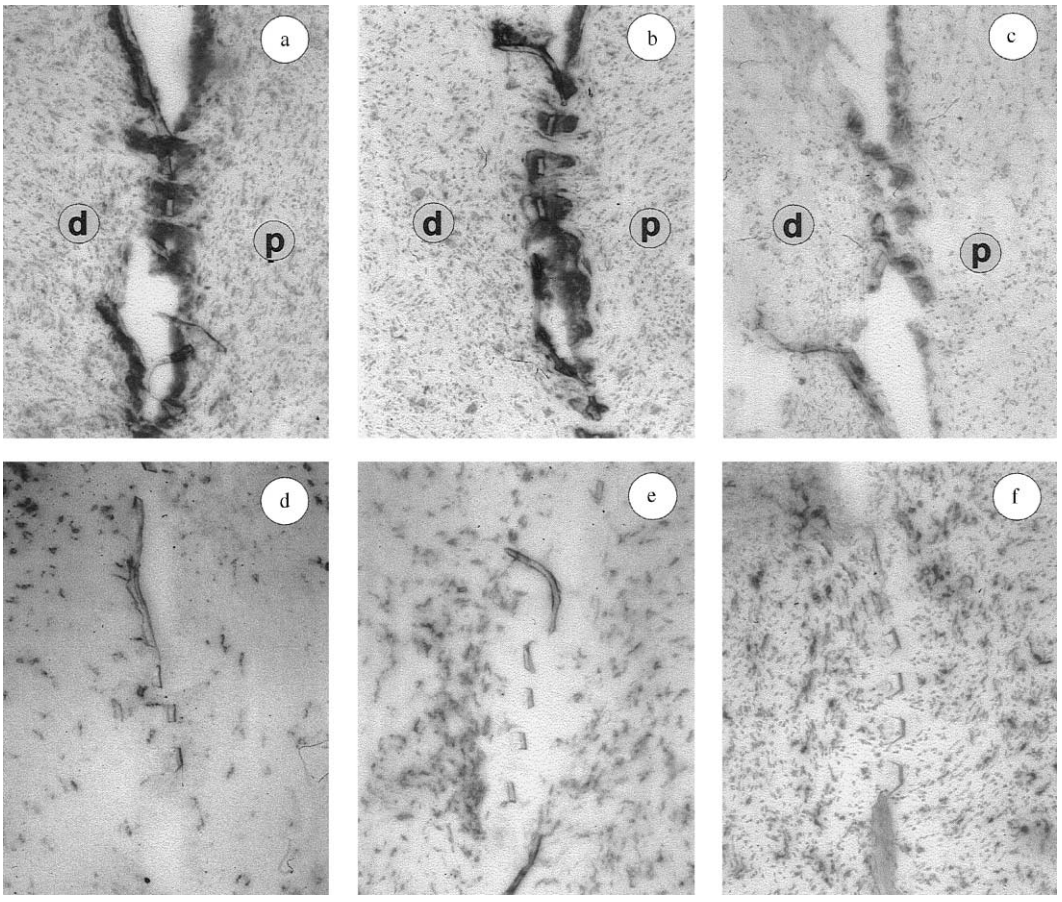

Fig. 7. Immunostaining of transverse sections of sieve electrode–nerve complex five weeks (a, d), six (b, e), and 11 months (c, f) after implantation with anti-CD11b (a–c) and ED2 (d–f) antibodies. CD11b-reactive hematogenous macrophages were found in direct contact with the sieve electrode. After an initial up-regulation after five weeks (a) and six months (b), the number and the intensity of stained cells substantially decreased 11 months (c) after implantation. The number of ED2-positive tissue resident macrophages did not display a significant alteration during time. Magnification 98 ×; p: proximal nerve stump, d: distal neuroma.

Parallel to this increase was the number of intensely labeled myelin-forming Schwann cells as shown by anti-Po-immunostaining (Figs. 5c, d and 6c, d). Compared to short-term implantation (Fig. 4d), Po was more frequently found in association with mature circular myelin sheath figures (Fig. 6d, arrows). The number of non-myelin-forming Schwann cells seemed to stagnate (Figs. 5e, f and 6e, f). However, the relative distribution of these cells was altered. Compared to short-term implantation where non-myelin-forming Schwann cells, like Po-positive Schwann cells and neurites were located within the center of each via hole (Figs. 3f and 4f), 11 months after implantation, non-myelin-forming Schwann cells were predominantly found at the periphery of each microfascicle (Fig. 5e, f, arrow, Fig. 6e, f, arrow), implying that a sort of segregation of both fiber types had occurred. Immunstaining for neurofilament and Schwann cell markers six months after implantation revealed an intermediate state with regard to neurite growth through the sieve electrode. Due to limitations of space these data have not been included in the present report.

3.2.2. Reactive tissue changes

To test the biocompatibility of the sieve electrode during long-term implantation, we focused on those cells that established direct contact with the polyimide implant. As described above, neurites and accompanying Schwann cells were only rarely found in contact with the sieve electrode but crossed the via holes in their center (Figs. 3a, b, 4a, b, 5a, b, 6a, b). To confirm our speculation that the cells adhering to the sieve electrode might be macrophages, we used anti-CD11b- and ED2-antibodies reactive with hematogenous and tissue resident macrophages, respectively. Whereas the number of tissue-resident macrophages was not altered following implantation (Fig. 7d–f) hematogenous macrophages displayed a numerical increase after five weeks and six months (Fig. 7a and b) and were down-regulated after 11 months (Fig. 7c). Higher magnifications revealed that hematogenous macrophages covered the implant and maintained an intimate contact with it during the time period studied (Fig. 8a–c). However, at no time point were any signs of degradation of the implant observed.

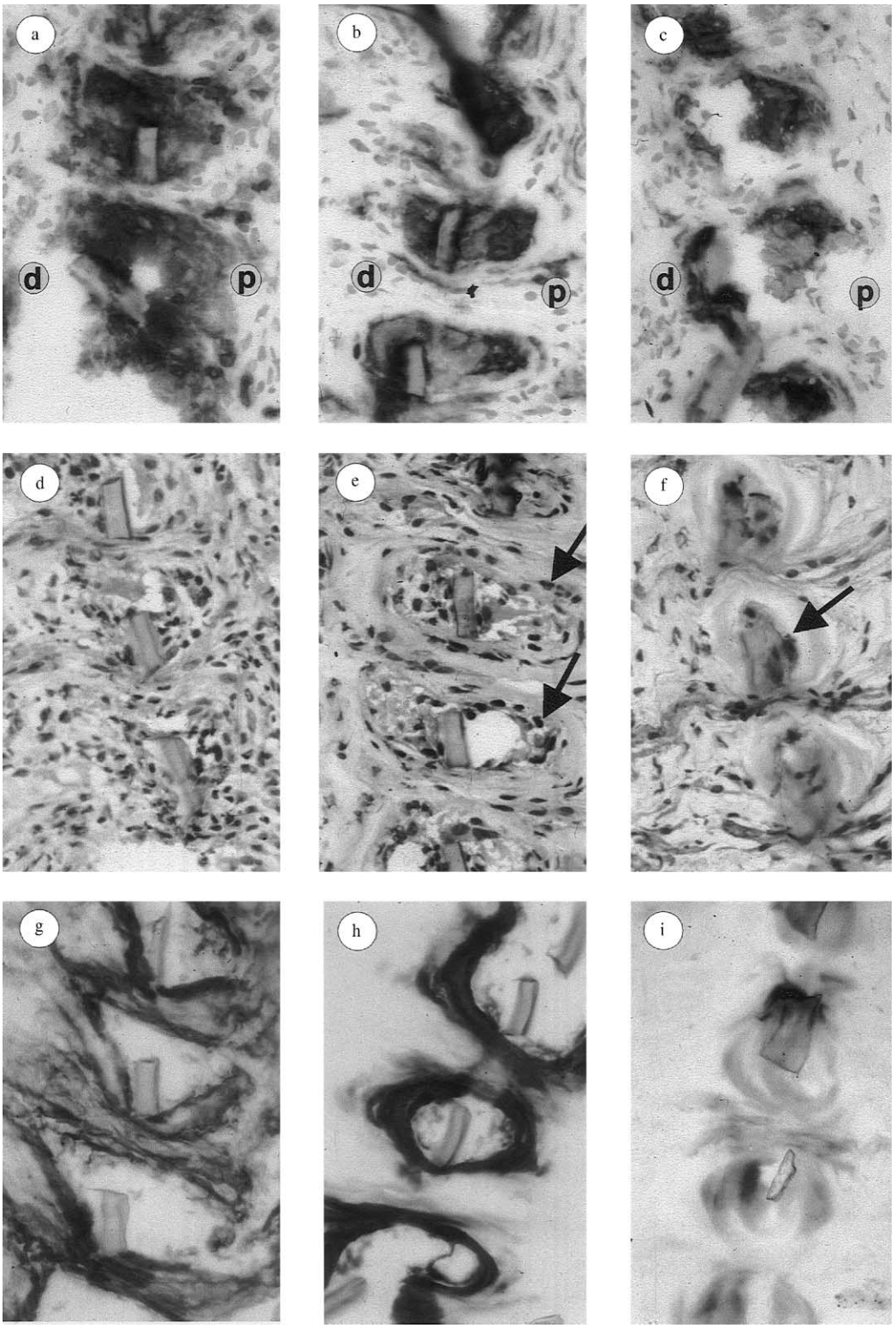

Fig. 8. High power photograph of transverse sections of the sieve electrode–nerve complex five weeks (a, d, g), six (b, e, h) and 11 (c, f, i) months after implantation stained with anti-CD11b-antibodies (a–c), hematoxylin/eosin (d–f), and the 10B3 monoclonal antibody. CD11b-reactive hematogenous macrophages (a–c) covered both the proximal and the distal face of the sieve electrode. Hematoxylin/eosin-counterstaining (d–f) revealed that after six and 11 months (e, f), hematogenous macrophages (e, f, arrows) resided inside hyaline acellular areas (e, f, arrows), which were strongly stained by the 10B3 monoclonal antibody reactive with a tenascin-C-like antigen (h, i). Staining of these structure drastically decreased from six (h) to 11 months (i). Contrary to long-term implantation (h, i), 10B3 immunostaining after five weeks was associated with fibers crossing the via holes. Magnification 390 ×; p: proximal nerve stump, d: distal neuroma.

Comparison with hematoxylin/eosin-stained sections (Fig. 8d–f) showed that the CD11b-positive macrophages after six and 11 months resided inside hyaline, acellular areas (Fig. 8e and f, arrows). These structures were stained by a monoclonal antibody (Fig. 8h and i) reactive with the tenascin-C like antigen 10B3 (Wewetzer et al., 1996; Wewetzer, unpublished). The 10B3 antigen after five weeks was strongly expressed and associated with fibers crossing the via holes as well as with structures surrounding the implanted electrode (Fig. 8g). Six months after implantation, the expression of 10B3 was still strong, but instead of an association with fibers crossing the via holes, the immunoreactivity was now found to be condensed in the cell-free structures surrounding CD11b-positive cells (Fig. 8h, f). Eleven months after implantation, 10B3 immunoreactivity had almost vanished, its localization, however, remained unchanged (Fig. 8i).

Table 1
Temporal expression of cell type-specific markers five weeks, six, and 11 months after implantation of the polyimide sieve electrode. Expression of the neuron- (neurofilament) and the myelin-specific (Po) markers steadily increased whereas the number of non-myelin-forming Schwann cell marker was not altered. Like 10B3, the expression of CD11b as a marker for hematogenous macrophages was high at five weeks and six months and decreased after 11 months. The expression of ED2 remained constant

Antigen	5 weeks	6 months	11 months
Neurofilament	+	+ +	+ + +
Po	+	+ +	+ + +
27C7	+	+	+
10B3	+ + +	+ +	±
CD11b	+ + +	+ + +	+
ED2	+	+	+

4. Discussion

Since integral electrodes of the peripheral nerve may be used for stimulation of grafted neurons thereby increasing their regenerative capacity, they hold great promise for the development of bioartificial nerve grafts improving the recovery of the peripheral nervous system after injury [15–17]. However, groups implanting such electrodes have predominantly focused on electrophysiological issues and there is only little data available concerning tissue-specific reactions in response to the electrode implantation at molecular terms [33–35]. Such a characterization is highly relevant for the subsequent use of electrodes since it might provide experimental evidence contributing to modified surgical procedures and/or electrode designs. In the present study we have aimed at a detailed qualitative analysis of axonal sprouting and reactive tissue changes after short- and long-term implantation of the electrode to the proximal stump of the transected adult rat sciatic nerve using cell type-specific antibodies.

4.1. Axonal sprouting through the sieve electrode

Immunostaining for neurofilament after short- and long-term implantation clearly demonstrated that the implanted sieve electrode permitted substantial axonal sprouting. Interestingly, the number of neurites crossing the via holes steadily increased from 5 weeks to 11 months (Table 1). The consistent sprouting through the electrode over the duration of 11 months is most likely due to a continuing fiber recruitment from the proximal nerve stump. The fact that axons crossed the sieve electrode is not intriguing and has already been shown by several other groups [36,35]. What was surprising, is the extent to which axons crossed the sieve electrode. After 11 months, between 20 and 40 neurites were observed to cross each via hole. Multiplying this number by the total number of via holes (657), it is speculated that approximately 19,000 neurites penetrated the sieve implant, which is the majority of the fibers found in the normal adult rat sciatic nerve [37,19,20]. Thus, we consider the "capacity" of the used electrode for ingrowing neurites sufficient for contacting peripheral nerves in a "physiological" manner. The present data are unable to show how many of these neurites were axonal branches known to be formed following transection injuries [38] and how many originated from distinct neurons. The possibility of retrograde sprouts re-entering the electrode from the distal neuroma can be considered negligible [26].

In order to characterize in more detail the fibers crossing the sieve electrode, we used cell type-specific antibodies against myelin-forming (Po) [30] and non-myelin-forming Schwann cells [31]. From the earliest time point studied (five weeks), both markers were found to be expressed by Schwann cells crossing the electrode and by cells of the distal neuroma (Table 1). Since expression of Po is dependent on axonal contact [39], it can be concluded that there was an intact neuron–Schwann cell interaction. Comparison of the staining pattern after short- and long-term implantation revealed two interesting features. Firstly, the number of myelin-forming Schwann cells was considerably increased, whereas the number of non-myelin-forming Schwann cells did not change. Secondly, five weeks after implantation, both Schwann-cell phenotypes were found intermingled with each other, whereas after 11 months, unmyelinated nerve fibers were localized to the periphery of each via hole. The numerical increase in Po-positive Schwann cells, paralleled by an increase in neurite number, together with the observation that the number of non-myelin-forming Schwann cells did not undergo further changes suggests that neurites were successively recruited from the proximal stump. The delayed recruitment of

Po-positive fibers might also explain the altered spatial distribution of myelinated and unmyelinated fibers observed after long-term implantation. Fine structural studies have revealed that myelinated and non-myelinated nerve fibers are not randomly associated in space but that there is a preferential relationship between groups of unmyelinated and myelinated fibers during development [40,27,41].

The expression of Po steadily increased over a period of 11 months. Fully differentiated Schwann-cell phenotypes with regular circular myelin sheath figures, however, were only observed after long-term implantation. It is known that Po during development is first detected in myelinating Schwann cells displaying 2–3 wrappings around the axonal processes [42]. We therefore conclude that myelination is initiated one month after implantation but not completed until 11 months following implantation.

4.2. Tissue-specific reactions at the nerve-electrode transitional area and the biocompatibility of the sieve implant

Cells that establish direct contact with the implant are of particular importance since they may contribute to degradation and therefore affect the stability and biocompatibility of the implant. Moreover, cells covering the implant may isolate neurites from the integral electrode array and therefore negatively affect both recording and stimulation properties of the electrode. As described above, myelinated and unmyelinated fibers were only rarely found in close contact with the sieve electrode but passed each via hole in its center. Previous studies on the biocompatibility of polymers have shown that macrophages adhere to the implant due to the hydrophilic or hydrophobic properties of the material [43]. It was shown that polyimide, as a typical hydrophilic polymer, is often associated with giant cell accumulations [44,45]. We therefore used anti-CD11b- and ED2-antibodies for localization of hematogenous and tissue-resident macrophages, respectively.

Hematogenous macrophages were found to be crowded at the proximal and distal surface of the sieve-interface five weeks and six months after implantation. This is not surprising since these so-called "crush macrophages" expressing the complement receptor III are usually found at the lesion site of transected or crushed nerves [28]. The accumulation of macrophages, therefore, is most likely a general reaction to nerve injury rather than a specific response to the implanted electrode. After long-term implantation, these macrophages were considerably down-regulated (Table 1) in number and were found in direct vicinity of the implant between via holes. Although CD11b-positive cells were in direct contact with the polyimide implant, no signs of phagocytotic activity or degradation either after short- or after long-term implantation of the implant were observed.

We observed hyaline, cell-free structures between hematogenous macrophages adhering to the sieve electrode and nerve fibers crossing the electrode six and 11 months after lesion. To further characterize these structures, we used monoclonal antibodies raised against Schwann cells [31,32]. The monoclonal antibody 10B3 was found to label these structures. 10B3 immunoreactivity after five weeks was associated with processes crossing the electrode and was subsequently observed in association with the cell-free areas. After 11 months, only residual immunoreactivity was observed, whereas the structures were still visible in hematoxylin/eosin staining. The 10B3 antigen displays an identical spatiotemporal distribution pattern as tenascin-C. The effects of tenascin-C with regard to the modulation of neurite growth are still controversial [46]. A number of studies have shown that domain-specific stimulation of neurite growth can be observed [47]. The present data might be interpreted as an indirect evidence for such a neurite growth-promoting activity of tenascin-C. During the initial phase of axonal sprouting (five weeks), strong expression of 10B3 was noted in Schwann cells and possibly fibroblasts invading from the epineurium. The fact that there was substantial down-regulation between six and 11 months (Table 1), although the number of crossing axonal processes further increased, may suggest that expression of tenascin-C-like antigens in Schwann cells is only necessary during the early phase. This, in turn, may add weight to the idea, that late sprouting myelinated fibers may use early growing fibers as guidance structures and therefore do not require the same expression level of growth-promoting molecules. The altered cellular distribution of 10B3 during this time might be explained by an initial presentation of the molecule on the surface of myelinating Schwann cells (one month), and the subsequent condensation at extracellular sites (six, 11 months) triggering removal of the antigen by macrophages.

In summary, our data clearly demonstrate that the introduced sieve electrode does not only permit substantial neurite growth but also displays a high degree of stability and biocompatibiltiy. Most relevant for the use of the electrode in electrophysiological experiments was the observation that the number of neurites and, therefore, the thickness of the microfascicles steadily increased over a period of 11 months whereas the number of macrophages covering the sieve electrode decreased. In future experiments we will use the introduced polyimide sieve electrode for the stimulation of neurons grafted to the peripheral nerve thereby increasing their regenerative potential.

Acknowledgements

The study was granted by the International Neurobionics Foundation (Hannover, Germany) and the

Bundesministerium für Bildung und Forschung (BMBF, BEO 11 0310880). We thank Dr. C. Grothe for providing anti-CD11b-antibodies and for helpful suggestions, N.v. Dornick for critical reading of the manuscript and I Heike for editorial help. Anti-Po-antibody was generously provided by Drs. Hartung and Archelos (Department of Neurology, University Graz, Austria).

References

[1] Fu SY, Gordon T. The cellular and molecular basis of peripheral nerve regeneration. Mol Neurobiol 1997;14:67–116.
[2] Goodrum JF, Bouldin TW. The cell biology of myelin degeneration and regeneration in the peripheral nervous system. J Neuropathol Exp Neurol 1996;55:943–53.
[3] Choi PD, Novak CB, Mackinnon SE, Kline DG. Quality of life and functional outcome of following brachial plexus injury. J Hand Surg [Am] 1997;22:605–12.
[4] Penkert G, Carvalho GA, Nikkhah G, Tatagiba M, Matthies C, Samii M. Diagnosis and surgery of brachial plexus injuries. J Reconstr Microsurg 1999;15:3–8.
[5] Samii M, Carvalho GA, Nikkhah G, Penkert G. Surgical reconstruction of the musculocutaneous nerve in traumatic brachial plexus injuries. J Neurosurg 1997;87:881–6.
[6] Samii M, Kahl RI. Klinische Resultate der autologen Nerventransplantationen. Med Mitt 1972;46:197–202.
[7] Fu SY, Gordon T. Contributing factors to poor functional recovery after delayed nerve repair: prolonged denervation. J Neurosci 1995;15:3886–95.
[8] Kline DG. Macroscopic and microscopic concomitants of nerve repair. Clin Neurosurg 1979;26:582–606.
[9] Kline DG, Judice DJ. Operative management of selected brachial plexus lesions. J Neurosurg 1983;58:631–49.
[10] Clowry GJ, Sieradzan K, Vrbova G. Grafts of embryonic tissue into spinal cord: a possible strategy for treating neuromuscular disorders. Neuromuscul Disord 1991;1:87–92.
[11] Clowry GJ, Vrbova G. Observations on the development of transplanted embryonic ventral horn neurones grafted into adult rat spinal cord and connected to skeletal muscle implants via a peripheral nerve. Exp Brain Res 1992;91:249–58.
[12] Demierre B, Ruiz-Flandes P, Martinou JC, Kato AC. Grafting of embryonic motoneurons into adult spinal cord and brain. Prog Brain Res 1990;82:233–7.
[13] Erb DE, Mora RJ, Bunge RP. Reinnervation of adult rat gastrocnemius muscle by embryonic motoneurons transplanted into the axotomized tibial nerve. Exp Neurol 1993;124:372–6.
[14] Katsuki M, Atsuta Y, Hirayama T. Reinnervation of denervated muscle by transplantation of fetal spinal cord to transected sciatic nerve in the rat. Brain Res 1997;771:31–6.
[15] Jellema T, Teepen JL. A miniaturized cuff electrode for electrical stimulation of peripheral nerves in the freely moving rat. Brain Res Bull 1995;37:551–4.
[16] Loeb GE, Peck RA. Cuff electrodes for chronic stimulation and recording of peripheral nerve activity. J Neurosci Methods 1996;64:95–103.
[17] Navarro X, Calvet S, Rodriguez FJ, Stieglitz T, Blau C, Buti M, Valderrama E, Meyer J-U. Stimulation and recording from regenerated peripheral nerves through polyimide sieve electrodes. J Peripheral Nervous System 1998;3:91–101.
[18] Stieglitz T, Beutel H, Meyer J-U. A flexible, light-weighted, multichannel sieve electrode with integrated cables for interfacing regenerating peripheral nerves. Sensors Actuators 1997;A60:240–3.
[19] Schmalbruch H. Fiber composition of the rat sciatic nerve. Anat Rec 1986;215:71–81.
[20] Swett JE, Torigoe Y, Elie VR, Bourassa CM, Miller PG. Sensory neurons of the rat sciatic nerve. Exp Neurol 1991;114:82–103.
[21] Swett JE, Wikholm RP, Blanks RH, Swett AL, Conley LC. Motoneurons of the rat sciatic nerve. Exp Neurol 1986;93:227–52.
[22] Richardson Jr RR, Miller JA, Reichert WM. Polyimides as biomaterials: preliminary biocompatibility testing. Biomaterials 1993;14:627–35.
[23] Mosconi T, Kruger L. Fixed-diameter polyethylene cuffs applied to the rat sciatic nerve induce a painful neuropathy: ultrastructural morphometric analysis of axonal alterations. Pain 1996;64:37–57.
[24] Stieglitz T, Beutel H, Schuettler M, Meyer J-U. Micromachined, polyimide-based devices for flexible neural interfaces. Biomed Microdev 2000;2:283–94.
[25] Navarro X, Verdu E, Buti M. Autotomy prevention by amitriptyline after section in different strains of mice. Restor Neurol Neurosci 1994;6:151–7.
[26] Amir R, Devor M. Ongoing activity in neuroma afferents bearing retrograde sprouts. Brain Res 1993;630:283–8.
[27] Fugleholm K, Toft PB, Schmalbruch H. Topography of unmyelinated axons in regenerated soleus nerves of the rat. J Neurol Sci 1992;109:25–9.
[28] Monaco S, Gehrmann J, Raivich G, Kreutzberg GW. MHC-positive, ramified macrophages in the normal, and injured rat peripheral nervous system. J Neurocytol 1992;21:623–34.
[29] Taskinen HS, Röyttä M. The dynamics of macrophage recruitment after nerve transection. Acta Neuropathol 1997;93:252–9.
[30] Archelos JJ, Roggenbuck K, Schneider-Schaulies J, Linington C, Toyka KV, Hartung H-P. Production and characterization of monoclonal antibodies to the extracellular domain of P0. J Neurosci Res 1993;35:46–53.
[31] Wewetzer K, Grothe C, Christ B, Seilheimer B. Identification and characterization of differentiation-dependent Schwann cell surface antigens by novel monoclonal antibodies: introduction of a marker common to the non-myelin-forming phenotype. GLIA 1997;19:213–26.
[32] Wewetzer K, Heiniger C, Seilheimer B. An improved cell ELISA for the differential screening of antibodies against cell surface molecules of viable adherent Schwann cells. J Immunol Methods 1996;191:171–8.
[33] Bradley RM, Cao X, Akin T, Najafi K. Long term chronic recordings from peripheral sensory fibers using a sieve electrode array. J Neurosci Methods 1997;73:177–86.
[34] Gonzalez C, Rodriguez M. A flexible perforated microelectrode array probe for action potential recording in nerve and muscle tissues. J Neurosci Methods 1997;72:189–95.
[35] Kovacs GT, Storment CW, Halks-Miller M, Belczynski Jr CR, Della Santina CC, Lewis ER, Maluf NI. Silicon-substrate microelectrode arrays for parallel recording of neural activity in peripheral and cranial nerves. IEEE Trans Biomed Engng 1994;41:567–77.
[36] Bradley RM, Smoke RH, Akin T, Najafi K. Functional regeneration of glossopharyngeal nerve through micromachined sieve electrode arrays. Brain Res 1992;594:84–90.
[37] Jenq CB, Chung K, Coggeshall RE. Postnatal loss of axons in normal rat sciatic nerve. J Comput Neurol 1986;244:445–50.
[38] Toft PB, Fugleholm K, Schmalbruch H. Axonal branching following crush lesions of peripheral nerves of rat. Muscle Nerve 1988;11:880–9.
[39] Lemke G, Chao M. Axons regulate Schwann cell expression of the major myelin and NGF receptor genes. Development 1988;102:499–504.
[40] Allt G. Ultrastructural features of the immature peripheral nerve. J Anat 1969;105:283–93.
[41] Webster HD. The geometry of peripheral myelin sheaths during their formation and growth of rat sciatic nerves. J Cell Biol 1971;48:348–67.

[42] Wiggins RC, Benjamins JA, Morell P. Appearance of myelin proteins in rat sciatic nerve during development. Brain Res 1975;89:99–106.
[43] Imai Y, Watanabe A, Masuhara E. Structure–biocompatibility relationship of condensation polymers. J Biomed Mater Res 1983;17:905–12.
[44] Pol BJ, van Wachem PB, van Luyn MJ, van der Does L, Bantjes A. In vivo testing of crosslinked polyethers. I. Tissue reactions and biodegradation. J Biomed Mater Res 1996;32:307–20.
[45] Schmidt S, Horch K, Normann R. Biocompatibility of silicon-based electrode arrays implanted in feline cortical tissue. J Biomed Mater Res 1993;27:1393–9.
[46] Faissner A. The tenascin gene family in axon growth and guidance. Cell Tissue Res 1997;290:331–41.
[47] Götz B, Scholze A, Clement A, Joester A, Schütte K, Wigger F, Frank R, Spiess E, Ekblom P, Faissner A. Tenascin-C contains distinct adhesive, anti-adhesive, and neurite outgrowth promoting sites for neurons. J Cell Biol 1996;132:681–99.